Chemosphere 266 (2021) 128950

Contents lists available at ScienceDirect

Chemosphere

journal homepage: www.elsevier.com/locate/chemosphere

Observable carbon isotope fractionation in the photodegradation of polybrominated diphenyl ethers by simulated sunlight

Zihe Ren [a, b], Yanhong Zeng [a, c, *], Xiaojun Luo [a, c], Chenchen Huang [a, b], Yankuan Tian [a, c], Shutao Gao [a, c], Bixian Mai [a, c]

[a] State Key Laboratory of Organic Geochemistry and Guangdong Provincial Key Laboratory of Environmental Protection and Resources Utilization, Guangzhou Institute of Geochemistry, Chinese Academy of Sciences, Guangzhou, 510640, People's Republic of China
[b] University of Chinese Academy of Sciences, Beijing, 100049, People's Republic of China
[c] Guangdong-Hong Kong-Macao Joint Laboratory for Environmental Pollution and Control, Guangzhou Institute of Geochemistry, Chinese Academy of Sciences, Guangzhou, 510640, People's Republic of China

HIGHLIGHTS

- Carbon isotope fractionation during the photolysis of PBDEs was investigated.
- Alterations to $\delta^{13}C$ values are further proof of the photodegradation of PBDEs.
- Diverse $\delta^{13}C$ values of products agree with different PBDE photolysis activities.
- Higher fractionation was observed for penta-BDEs than for hexa-BDEs.

ARTICLE INFO

Article history:
Received 28 August 2020
Received in revised form
3 November 2020
Accepted 10 November 2020
Available online 13 November 2020

Handling Editor: Keith Maruya

Keywords:
Polybrominated diphenyl ethers
Photodegradation
Carbon isotope fractionation
Simulated sunlight irradiation

ABSTRACT

In the present study, carbon isotope effects were investigated during the photodegradation of polybrominated diphenyl ethers (PBDEs) by compound-specific stable isotope analysis (CSIA). Five PBDE congeners (BDE 85, 99, 100, 153 and 154) in n-hexane were individually exposed to simulated sunlight for as long as 15 h, except for BDE 100 (24 h). Consecutive debromination of PBDE by photolysis in n-hexane was confirmed by the clear ^{13}C enrichment of mother congeners and successive depletion of $\delta^{13}C$ values for the photodegradation products with decreasing degree of bromination, which can be attributed to mass-dependent isotope fractionation. The observed variation in the isotope fractionation trends for the *para*-debrominated products might be linked to the different photocatalytic activities of the PBDE congeners. Higher fractionation was observed for penta-BDEs ($\varepsilon_{C=}$ −2.2 ± 0.45‰ and −2.3 ± 0.26‰ for BDE 85 and BDE 99, respectively) compared to that for hexa-BDEs ($\varepsilon_{C=}$ −1.7 ± 0.41‰, and −1.3 ± 0.12‰ for BDE 153 and BDE 154, respectively). Normal isotope effects (AKIE > 1) observed in our study supports the utility of CSIA for the evaluation of the photodegradation of PBDEs.

1. Introduction

Polybrominated diphenyl ethers (PBDEs), brominated flame retardants, have been extensively used in various consumer products over the past four decades (Besis and Samara, 2012). The widespread use of PBDEs has made them prevalent in the environment (Li et al., 2016; Wang et al., 2016; Gandhi et al., 2017; Li et al., 2017; Morris et al., 2018). It is known that PBDEs bioaccumulate and lead to adverse effects for sensitive human populations, such as indigenous people and fish consumers, and for some wildlife (de Wit, 2002). As a result of their harmful characteristics, PBDEs are on the radar of environmental authorities (e.g., Stockholm Convention). Penta-BDE and Octa-BDE commercial mixtures were officially classified as persistent organic pollutants (POPs) and included in the Annex A of the Stockholm Convention in 2009, and Deca-BDE was included in 2017 (Commission 2017). Despite these efforts, human and environment exposure has continued for decades due to the big "reservoir" of existing

* Corresponding author. State Key Laboratory of Organic Geochemistry and Guangdong Provincial Key Laboratory of Environmental Protection and Resources Utilization, Guangzhou Institute of Geochemistry, Chinese Academy of Sciences, Guangzhou, 510640, People's Republic of China.
E-mail address: zengyh@gig.ac.cn (Y. Zeng).

https://doi.org/10.1016/j.chemosphere.2020.128950
0045-6535/

products containing PBDEs. It has been estimated that, in 2018, the global in-use and waste stocks of PBDEs (BDE 28, 47, 99, 153, 183, and 209) were approximately 425 000 tons and 113 000 tons, respectively, (Abbasi et al., 2019). Therefore, significant environmental concerns have been raised through studies of the behavior and fate of PBDEs in the environment, such as biodegradation (Wang et al., 2018b), photodegradation (Wang et al., 2018a), and advanced oxidation processes (Feo et al., 2014).

Among the relevant chemical processes, photodegradation is an important process for the natural attenuation of PBDEs, for which a stepwise debromination mechanism has been suggested (Pan et al., 2016). During the photolysis of PBDEs, less-brominated PBDE congeners and other derivatives gradually accumulate, some of which are more toxic and have greater bioaccumulation potential than the parent pollutants (Usenko et al., 2011; Bendig and Vetter, 2013; Zhao et al., 2015). Consequently, consideration of photodegradation of PBDEs is crucial to produce accurate risk assessments for PBDEs in the environment due to the more toxic degradation products relative to their mother compounds. Nonetheless, although numerous studies have investigated possible PBDE photodegradation mechanisms based on the identification of metabolites and degradation products (Pan et al., 2016), limited data for the identification and quantification of PBDE photodegradation at field scale are available. For the case of PBDEs, the identification of the photodegradation processes might be very difficult by concentration analysis because (i) a specific PBDE congener in the environment, or the product of higher brominated congeners, can be accumulated, and (ii) both photodegradation and nondegradation processes, such as volatilization or adsorption, can contribute to the attenuation of PBDEs in the environment.

Compound-specific isotope analysis (CSIA) using gas chromatography in combination with isotope ratio mass spectrometry (GC-C-IRMS) analysis has been shown to be a promising technique for the identification and quantification of transformation pathways for different organic contaminants (Schmidt et al., 2004). GC-C-IRMS has made it possible to separate organic compounds from complex mixtures and to determine their individual stable isotope ratios. CSIA utilizes minute mass-dependent effects due to the lower mobility and higher binding energies of heavier isotopes, resulting in an enrichment of heavy isotopes in the remaining substrate (e.g., normal isotope fractionation). This novel approach allows the measurement of bulk isotopic enrichment factors, ε_{bulk}, identifiers for linking the changes in isotope ratios to the transformation processes of the organic pollutants. To date, isotope fractionation during photodegradation of PBDEs has rarely been studied. Only one study has paid attention to carbon stable isotope fractionation in the UV photolysis of PBDEs and a ε_{bulk} value was obtained only for BDE 47 (Rosenfelder et al., 2011). Therefore, the goal of this study was to assess carbon isotope fractionation during the photodegradation process for PBDEs.

During normal isotope fractionation, the average carbon isotope value for the residual, nondegraded fraction of the contaminant molecular change can usually be described by the Rayleigh equation (Elsner et al., 2005). Therefore, the values for the enrichment factors (ε_C) for the degradation of a certain pollutant can be determined under representative conditions in a laboratory experiment according to the Rayleigh equation (see eq. (1)). Furthermore, by including the correction for nonreactive locations in the Rayleigh equation, position-specific enrichment factors ($\varepsilon_{reactive\ position}$) can be obtained, and by using these $\varepsilon_{reactive\ position}$ values, the apparent kinetic isotope effect (AKIE) for this position can be calculated (see eq. (2)) (Elsner et al., 2005). Principally, significant isotope fractionation can only be expected at those positions, where covalent bonds involving the element E, either directly or indirectly, are broken or formed during the rate-determining step for a given reaction (Elsner et al., 2005). If C—Br cleavage is a rate-limiting step during PBDE photodegradation, the carbon isotope effects are expected to be similar based on a comparison of the theoretical maximum kinetic isotope effects (KIEs) with a C-KIE of 1.040 (Zakon et al., 2013).

In this study, we chose five dominant congeners (BDE 85, 99, 100, 153, and 154) in a penta-BDE mixture as model compounds for PBDEs. The carbon isotope fractionation was investigated for the PBDEs in solutions treated by simulated sunlight. We determined the stable carbon isotope ratios ($\delta^{13}C$ values), enrichment factors (ε_C), and apparent kinetic isotope effects (AKIE) for the PBDEs and attempted to characterize the carbon isotope fractionation trends and evaluate them by comparing them with reports for brominated analogs. Estimates for the isotope fractionation during the photodegradation of PBDEs have rarely been reported. Therefore, our study tried to find the connection between isotope fractionation and possible reaction mechanism to characterize the photodegradation of PBDEs better.

2. Materials and methods

2.1. Chemicals and materials

Five PBDE congeners (BDE 85, 99, 100, 153, and 154) used for simulated solar degradation, a surrogate internal standard and recovery standard (BDE 77, 118, 205, 4-F-BDE 67, 3-F-BDE 153), and other PBDE standards mentioned in the present study were purchased from AccuStandard (New Haven, CT). All the standard compounds and stock solutions were prepared in isooctane. An artificial mixture was reconstituted in isooctane consisting of BDE 28, 47, 85, 99, 100, 153, and 154. This mixture was used as a daily correction to ensure stability for the GC-C-IRMS. Pesticide grade acetone (Ace), dichloromethane (DCM) and n-hexane (Hex) were purchased from CNW Technologies GmbH (Dusseldorf, Germany).

2.2. Photodegradation experiments

The photolytic experiments were performed in Hex according to previous reports (Fang et al., 2008; Wei et al., 2013). BDE standard solutions were placed into a 30 mL quartz glass vessel, which was placed around a 1000 W xenon lamp in a photoreactor (BL-GHX-V, Shanghai Bilon Instrument Co., Ltd. Shanghai, China). The lamp was placed into a quartz tank and surrounded by flowing water maintained at 26 ± 1 °C. For xenon light sources, eight quartz filters (13.5 cm × 3.5 cm × 0.2 cm) were used around the xenon lamp to remove the ultraviolet wavelengths below 290 nm to simulate sunlight irradiation. The filters were purchased from Shanghai Depai Biotech. Co. Ltd., China. The sampling points were set at 0/3/6/9/12/15 h for BDE 85, 99, 153, and 154, and 0/10/12/24 h for BDE 100. At each sampling time, 5 mL of solution was taken out and BDE 77 (1250 ng/μL × 10 μL) was added as a surrogate internal standard. The mixture was blown and evaporated to near dryness by gentle nitrogen gas flow. Then, 100 μL of isooctane was added to resolve the pollutants. Next, 10 μL of solution was taken out and 4-F-BDE 67 (2 ng/μL × 30 μL) and 3-F-BDE 153 (2 ng/μL × 30 μL) were added as internal standards prior to redissolution in 300 μL of isooctane for the PBDE analysis. The dark control samples were maintained inside the glass tube, wrapped in aluminum foil to protect them from light exposure. All the experiments were conducted in triplicate.

2.3. Instrument analysis

Quantitative analysis The PBDE congeners were quantified using a gas chromatograph/mass spectrometer (GC/MS) (Agilent 6890 N/5975B MSD; Agilent Technology, CA) with an electron-capture

negative chemical ionization (ENCI) source in selective-ion monitoring mode. GC separation was performed using a DB-XLB capillary column (30 m × 0.25 mm i. d. × 0.25 mm film thickness). The oven temperature program was set up as follows: 110 °C (held for 1 min), increased to 180 °C at 16 °C/min (held for 0.5 min), to 240 °C at 4 °C/min (held for 2.5 min), to 280 °C at 4 °C/min (held for 8 min), and finally to 305 °C at 20 °C/min (held for 10 min). All analytes were identified based on their retention times in the capillary columns and verified by matching retention times with authentic standard mixtures (39 PBDE congeners for photocatalytic degradation, obtained from AccuStandard). Quantification was performed using the internal calibration method based on a five-point calibration curve. Congeners that were not included in the authentic standards were quantitated using the relative response factors for the congener with the closest retention time for the synthetic standard.

Isotope analysis The purity of the extracts used for CSIA was first checked using an Agilent 7890 A GC-5975C MS system with an EI ion source in full-scan mode. In the present study, the $\delta^{13}C$ values for the PBDE congeners were analyzed by a Trace GC Ultra-IsoLink Delta V Advantage isotope ratio mass spectrometer (Thermo-Fisher Scientific, Waltham, MA, USA). Samples were injected at 290 °C in splitless mode. PBDEs were separated on a DB-5 MS capillary column (30 m × 0.25 mm i. d. × 0.25 μm film thickness). Helium was used as a carrier gas at a constant flow rate of 1.2 mL/min. The GC temperature was initially set to 70 °C (held for 1.5 min), increased to 230 °C at 30 °C/min (held for 0 min), then increased to 270 °C at 4 °C/min (held for 1 min), followed by an increase to 280 °C at 2 °C/min (held for 0.5 min), and finally, increased to 315 °C at 15 °C/min (held for 25 min). The combustion interface was maintained at a temperature of 1050 °C.

2.4. Calculations and evaluation of data

The carbon isotope enrichment factor (ε_C) was determined for PBDEs according to the Rayleigh equation (see eq. (1)) (Elsner et al., 2005):

$$\ln\frac{(1000+\delta^{13}C)}{(1000+\delta^{13}C_0)}\approx\frac{\varepsilon_C}{1000}lnf \quad (1)$$

where ε_C is the enrichment factor and denoted in permil, f is the residual substrate fraction at time t, and $\delta^{13}C$ and $\delta^{13}C_0$ are the isotope ratios at time t and time zero, respectively.

The apparent kinetic isotope effects (AKIE) for carbon for each debromination reaction were estimated using the following equation (Elsner et al., 2005):

$$AKIE_C=\frac{1}{1+z\times\varepsilon_{reactive\ position}/1000} \quad (2)$$

where z is the number of atoms in intramolecular competition, and $\varepsilon_{reactive\ position}$ is the reactive position-specific ε, which can be calculated as follows (Elsner et al., 2005):

$$\varepsilon_{reactive\ position}=\varepsilon_C\times\frac{n}{x} \quad (3)$$

where ε_C is the bulk enrichment, n is the number of atoms of carbon considered in the molecule, and $x$is the number of atoms of carbon considered at the reactive site. Assuming the debromination occurs step wise and for primary isotope effects $z = x$, the AKIE value can be estimated by

$$AKIE_C=\frac{1}{1+n\times\varepsilon_C/1000} \quad (4)$$

2.5. Statistical analysis

All data are presented as the means ± standard deviations unless otherwise specified. Origin 9.1 software was used for statistical analysis and graph drawing. The photolysis rate constants (k) were determined via linear fitting between sampling times and the remaining ratio for the substrates. A level of significance of 5% was retained.

3. Results and discussion

3.1. Reaction kinetics and products of PBDE photodegradation

A control experiment was conducted for the PBDE congeners studied in the present study. No degradation of PBDEs was observed in the dark control samples, indicating that only simulated sunlight can degrade PBDEs. Upon irradiation of the mother PBDE congeners with simulated sunlight, the loss of PBDEs increased with reaction time. As shown in Figure S1, the kinetics for the degradation all mother PBDEs in n-hexane can be fitted well by a pseudo first-order model. The first order rate constant for the degradation of a mother congener was obtained from the slopes of $-\ln(C_t/C_0)$ versus exposure time (Figure S1), where C_t and C_0 are the concentration of mother congeners at a given time t (h) and the initial concentration, respectively. The photodegradation rate constants for the five mother congeners followed the order of BDE 153 (245-245) (0.13 h^{-1}) > BDE 99 (245–24) (0.09 h^{-1}) >BDE 85 (234–24) (0.08 h^{-1}) > BDE 154 (245–246) (0.07 h^{-1}) >BDE 100 (246–24) (0.007 h^{-1}) (Table 1). The photodegradation rate trends observed in the present study are in agreement with the findings of previous studies (Mas et al., 2008; Wei et al., 2013). In general, the higher brominated congeners show higher first order removal rates compared to the less-brominated congeners, and the much lower degradation rates found for BDE 154 and BDE 100 may be attributed to the more stable brominated phenyl ring with 2,4,6-substitution in BDE 154 and BDE 100 (Pan et al., 2016).

Figure S2 shows the concentration of the mother BDE congeners and their photoproducts at different irradiation times. We found that the dominant products (BDE 47 from BDE 85; BDE 47 and BDE 66 from BDE 99; BDE 99 and BDE 118 from BDE 153; BDE 100 from BDE 154; and BDE 75 and BDE 47 from BDE 100) were generally formed by the loss of a bromine atom from the *ortho* and *meta* positions. Tri- (BDE 28, BDE 37) and di- (BDE 15) homologs were also detected by GC-MS. The degradation profiles obtained for PBDEs analyzed in our study are in agreement with the findings of Pan (Pan et al., 2016). Although the total molar mass of the PBDEs before and after the photolysis reaction was not balanced, for the these congeners (BDE 85, 99, 100, 153, and 154), more than 70% of the original molar mass of the PBDEs was left over after 24 h of irradiation (Figure S3), which is much higher than that reported for higher brominated congeners (less than 31% for BDE 209, 208, and 206) after 4 h of exposure to sunlight (Wei et al., 2013). This suggests that debromination is the dominant mechanism for the photolysis of penta and hexa homologs in n-hexane.

3.2. Changes in the stable isotope ratios for PBDEs during photodegradation

In the present study, approximately 16 PBDEs were identified

Table 1
The rate constants, half-lives, $\delta^{13}C$ values, isotope enrichment factors ε_C and AKIE values for the PBDE congeners during the photodegradation.

	Rate constants (k, h^{-1})	Half-life ($t_{1/2}$, h)	$\delta^{13}C_0$ (‰)[a] (t = 0 h)	$\delta^{13}C_d$ (‰)[b] (dark samples)	$\Delta\delta^{13}C_d$ (‰)[c]	$\delta^{13}C_s$ (‰)[d] (t = 15/24 h)	$\Delta\delta^{13}C_s$ (‰)[e]	ε_C	AKIE
BDE 85	0.08	8.75	−28.57 ± 0.04	−28.82 ± 0.03	−0.25	−26.50 ± 0.43	2.07	−2.2 ± 0.45	1.027 ± 0.006
BDE 99	0.09	7.71	−32.11 ± 0.13	−31.95 ± 0.19	0.16	−29.18 ± 0.39	2.93	−2.3 ± 0.26	1.029 ± 0.003
BDE 153	0.13	5.25	−31.70 ± 0.00	−32.06 ± 0.07	−0.36	−28.66 ± 0.28	3.04	−1.7 ± 0.41	1.023 ± 0.005
BDE 154	0.07	10.10	−30.85 ± 0.02	−30.64 ± 0.12	0.21	−29.17 ± 0.20	1.68	−1.3 ± 0.12	1.015 ± 0.001
BDE 100	0.007	93.04	−31.88 ± 0.02	−31.67 ± 0.18	0.21	−31.88 ± 0.27	0.00	–	–

[a] $\delta^{13}C$ values for five PBDE congeners at time t = 0 h.
[b] $\delta^{13}C$ values for the dark samples for five PBDE congeners at time t = 15 h for BDE 85, 99 153, and 154, t = 24 h for BDE 100.
[c] $\Delta\delta^{13}C_d$ (‰) = $\delta^{13}C_d$ - $\delta^{13}C_0$.
[d] $\delta^{13}C$ values for five PBDE congeners at the end of the irradiation, t = 15 h for BDE 85, 99 153, and 154, and t = 24 h for BDE 100.
[e] $\Delta\delta^{13}C_s$ (‰) = $\delta^{13}C_s$ - $\delta^{13}C_0$.

with GC-MS, while stable carbon isotope ratios ($\delta^{13}C$, ‰) could only be determined for the most abundant thirteen PBDE congeners (Fig. 1, Table S1). As shown in Fig. 1f and Table 1, no significant carbon isotope fractionation ($|\Delta\delta^{13}C| < 0.5$‰) was observed for the five mother PBDE congeners at time t = 0 h and t = 15/24 h for the dark samples (time 15 h for BDE 85/99/153/154, and time 24 h for BDE 100), indicating that only photodegradation can lead to the carbon isotope fractionation of PBDEs.

Clear ^{13}C enrichments (less-negative $\delta^{13}C$ values) were observed for the four mother PBDE congeners (BDE 85, 99, 153, and 154), while relatively constant $\delta^{13}C$ values were observed for BDE 100 over time (Fig. 1a–e, Table S1). These trends are consistent with the steady decrease in the concentration of the four mother congeners and a virtually constant amount of BDE 100 throughout the irradiation process (Fig. S2), confirming that the observed fractionation is associated the photolysis of the PBDEs. The $\delta^{13}C$ values for the first major transformation products of the same mother congeners were found to be different (Fig. 1a–d, Table S1). Generally, these values were lower than those obtained for the corresponding mother congeners and showed a steady increase in the ^{13}C content over time, except for the products BDE 103 and BDE 99 of BDE 154 (Fig. 1d). The further transformation of these first products can make them heavier in carbon, as supported by the simultaneous detection of tri- or tetra-BDEs during the irradiation (Fig. S2). However, the $\delta^{13}C$ values for the BDE 103 product of BDE 154 remained constant and generally similar to the $\delta^{13}C$ value obtained for BDE 154 before irradiation with increasing concentration throughout the irradiation process (Fig. 1d and Fig. S2). This phenomenon is likely due to the formation and transformation resulted coincidently in a constant $\delta^{13}C$ values of BDE 103; similar findings

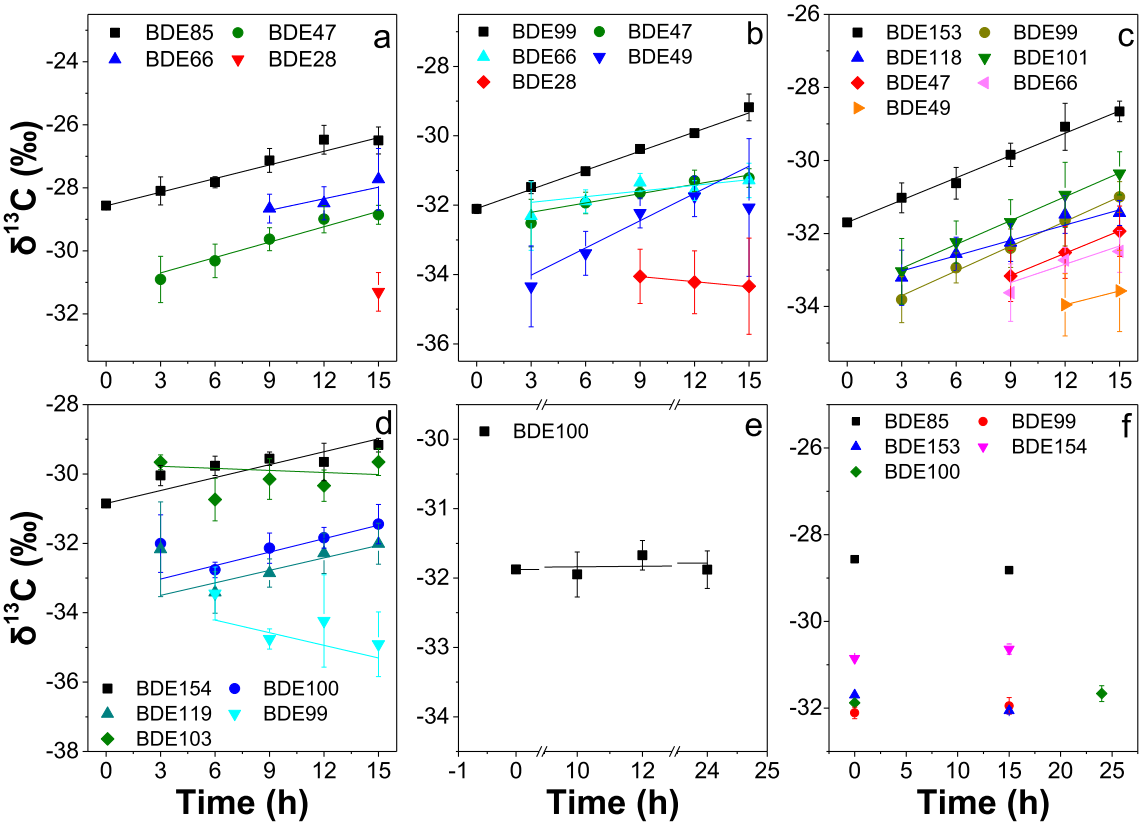

Fig. 1. $\delta^{13}C$ values for five PBDE congeners and their photodegradation products over time. (a), (b), (c), (d), and (e) represent the measurable changes in the isotopes of the photolysis process for BDE 85/99/153/154/100, respectively. (f) Comparison between the $\delta^{13}C$ values obtained for the five mother PBDE congeners at time t = 0 h and t = 15/24 h for the dark samples (for BDE 85/99/153/154 at time 15 h, for BDE 100 at time 24 h).

were also reported in a previous study. Rosenfelder et al. observed a constant $\delta^{13}C$ value for BDE 28, which was similar to that obtained for the mother congener BDE 47 before irradiation (Rosenfelder et al., 2011).

In contrast, compared to the first major transformation products (BDE 119, 100, and 103) of BDE 154, the first minor product, BDE 99, became lighter in carbon during the course of the irradiation. Isotope effects generally become larger as the bond strength is changed between the photophysical excitation and relaxation processes (Elsner et al., 2005). Notably, BDE 99 (245–24) was formed by the loss of a bromine atom from the more stable brominated phenyl ring with a 2,4,6-substitution in BDE 154 (245–246), while the other three dominant products (BDE 119 (34–246), BDE 100 (24–246), and BDE 103 (25–246)) were all formed by the loss of one bromine atom from the less stable ring (245-substitution) of BDE 154. Therefore, the significant decreasing trend in the ^{13}C content of BDE 99 relative to the mother congener, BDE 154, is presumably associated with the cleavage of a C–Br bond in the stable ring with the 2,4,6-substitution in BDE 154. A more detailed elucidation of the reaction mechanisms for such a stable brominated phenyl ring for the isotope fractionation of BDE 99 cannot be assessed from the available literature and requires further study. As expected, the $\delta^{13}C$ values for the second major products (BDE 66, BDE 49, BDE 47, and BDE 28) were significantly depleted relative to those for the first major products (BDE 118, BDE 101, and BDE 99 in Fig. 1c; BDE 66, BDE 49, and BDE 47 in Fig. 1b). In addition, the second debromination products (BDE 66, BDE 49, and BDE 47) for BDE 153 exhibited clear ^{13}C enrichment trends during the course of irradiation (Fig. 1c). In contrast, the second major products BDE 28 of BDE 99 became lighter in carbon over time (Fig. 1b). Because of the increasing stability of PBDEs with decreasing degree of bromination (Bendig and Vetter, 2010), the greater persistence of BDE 28 relative to BDE 66, BDE 49, and BDE 66 is consistence with a decreasing trend for the $\delta^{13}C$ values (Rosenfelder et al., 2011). Moreover, these second debromination products can be formed from the debromination from different first debromination products (e.g., BDE 49 from BDE 99 and BDE 101; BDE 28 from BDE 47 and BDE 66). Therefore the multiple sources with different isotope composition of these second debromination products can also be a possible reason for the observed different ^{13}C enrichment trends. Our dataset does not allow a detailed interpretation here. For further insights into the connection between photodegradation processes and the isotope fractionation of PBDEs, a multielement (C, Br) approach might help.

It is also interesting to observe that both the first and the second *para*-debrominated product (BDE 49, tetra-BDE) of the mother congeners BDE 99 and BDE 153, respectively, was much more depleted in ^{13}C compared to the *meta*-/*ortho*-debrominated products (BDE 47 and BDE 66) of the same mother congeners (Fig. 1b–c). However, the *para*-debrominated penta-BDE products of the hexa-BDEs (BDE 101 (245–25) of BDE 153 (245-245) and BDE 103 (25–246) of BDE 154 (245–246)) showed higher $\delta^{13}C$ values compared to the *meta*-/*ortho*-debrominated products converted from the same precursor PBDEs (Fig. 1c–d). The identity of the origin of the isotope fractionation associated with position-specific and degree of bromination during the photolysis of PBDEs remains unknown, but our data offer room for interesting speculation. Obviously, these *para*-/*meta*-/*ortho*-debrominated products can be decomposed and formed during the irradiation, and these processes lead to their enrichment and depletion of carbon isotope composition, respectively. In addition, the $\delta^{13}C$ values for these products were associated with both the amount of these products formed and decomposed during the irradiation. It means that if the congeners are mainly formed while their decomposition is slow, they likely become lighter in carbon; on the contrary, if their further degradation is also evidence, depletion in ^{13}C will be masked to a certain extent. As mentioned earlier, previous studies have demonstrated that the stability of PBDE congeners is increased as the degree of bromination increases (Bendig and Vetter, 2010). Therefore, the above mentioned different isotope variation between the different degree of bromination *para*-debrominated products and *meta*-/*ortho*-debrominated products of the same mother congeners might be linked with the greater stability of BDE 49 (tetra-BDE) compared to BDE 101 (penta-BDE) and BDE 103 (penta-BDE).

As previously found for PCBs and PBDEs, the $\delta^{13}C$ values for individual congeners become more negative as the degree of halogenation is increased (Jarman et al., 1998; Vetter et al., 2008). Therefore, to determine the impact of the degree of bromination on the $\delta^{13}C$ values, we plotted the $\delta^{13}C$ values vs. the degree of bromination. For each sample, only the $\delta^{13}C$ values for the PBDE congeners available when the degree of bromination varied by a factor larger than two were investigated (Figure S4). Approximate parallel linear regressions were found for the different irradiated mother congeners, and the slopes ranged from 1.6 to 2.5 for the three irradiated congeners (BDE 85, BDE 99, and BDE 153), in agreement with the finding (slope = 2.0 and 2.4 for the irradiation of BDE 47) from a previous study (Rosenfelder et al., 2011). Thus, our findings further support the application of slopes to predict $\delta^{13}C$ for the minor photodegradation products of PBDEs under laboratory control conditions, and the slopes may be used as a possible basis for the assessment of PBDEs originating from UV-induced hydro-debromination.

3.3. Evaluation of the photodegradation from isotope fractionation

The Rayleigh equation was used to evaluate the observed isotopic fractionation. As shown in Fig. 2, the enrichment in ^{13}C isotope composition and the decrease in PBDE concentration were linear in the double logarithmic Rayleigh plot. From these Rayleigh plots ($R^2 \geq 0.72$, Fig. 2), the enrichment factors ε_C for BDE 85, BDE 99, BDE 153, and BDE 154 were determined to be $-2.2 \pm 0.45‰$, $-2.3 \pm 0.26‰$, $-1.7 \pm 0.41‰$, and $-1.3 \pm 0.12‰$, respectively (Table 1). These observed carbon isotope effects are comparable to the value of $\varepsilon_C = -2.11 \pm 0.45‰$ reported for the UV-debromination of BDE 47 (tetra-BDE) by Rosenfelder et al. (2011). The enrichment factors, ε_C, were then used to calculate the apparent kinetic isotope effect ($AKIE_C$) values. According to eq. (4), the $AKIE_C$

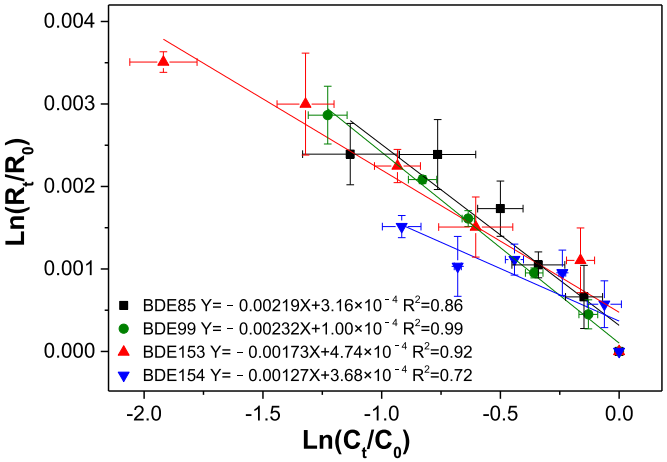

Fig. 2. Rayleigh plots for carbon stable isotope fractionation of four obviously degraded PBDE congeners. R_0 is the initial isotopic ratio and R_t is the isotopic ratio of the compound at time t.

values for BDE 85, BDE 99, BDE 153, and BDE 154 were calculated to be 1.027 ± 0.006, 1.029 ± 0.003, 1.023 ± 0.005, and 1.015 ± 0.001, respectively (Table 1). Comparable literature values for $AKIE_C$ ranging between 1.016 and 1.023 were observed for C–Br bond cleavage from brominated phenols (Zakon et al., 2013). Although these values are below the Semiclassical Streitweiser Limits for $AKIE_C$ of C–Br bond cleavage (1.040) (Zakon et al., 2013), they are still of the same order of magnitude expected for such a process occurring as a key reaction step. This can be attributed to the incomplete expression of C–Br bond fission used for the KIE_C calculated by Semiclassical Streitwieser Limits, which usually takes into account only differences in vibrational energies and assumes that the bond is completely broken in the excited state (Zelmer et al., 2015). Therefore, if one takes the different nature of the transition state into account, these values are not unexpected.

4. Conclusion

Our study investigated the carbon isotope fractionation associated with the photolysis of PBDEs. Consecutive debromination is the dominant mechanism underlying PBDE photolysis in n-hexane, and the processes were confirmed by the observation of steady alterations in the $\delta^{13}C$ values for the PBDEs. The $\delta^{13}C$ values obtained for the photodegradation products of the PBDEs were found to decrease with decreasing degree of bromination. A difference in the isotope fractionation trends was observed for the intermediate products, which is likely linked to the different photocatalytic activities of the PBDE congeners. The photodegradation for the tested PBDEs exhibited normal isotope effects (AKIE > 1), and strong carbon isotope effects were observed in our study, which supports the utility of CSIA for the evaluation of the photodegradation of PBDEs. Undoubtedly, more work is required to identify the origin of the isotope fractionation associated with the photocatalytic activities during the photolysis of PBDEs.

Credit author statement

Zihe Ren: experimenter, Formal analysis, Writing - original draft preparation, Validation, Formal analysis. Yanhong Zeng: Conceptualization, Resources, Writing - review & editing, Validation, Supervision, Project administration, and Funding acquisition. Xiaojun Luo: Conceptualization, Writing - review & editing, and Supervision. Chenchen Huang: Formal analysis and validation, Software. Yankuan Tian: Data curation, instrument acquisition. Shutao Gao, Data curation, instrument acquisition. Bixian Mai: Funding acquisition, Supervision.

Declaration of competing interest

The authors declare that they have no known competing financial interests or personal relationships that could have appeared to influence the work reported in this paper.

Acknowledgments

This work was supported by the National Natural Science Foundation of China (nos. 41977306 and 41773129), the Guangzhou Science and Technology Project (no. 202002030134), the Local Innovative and Research Teams Project of Guangdong Pearl River Talents Program (no. 2017BT01Z134), Guangdong Foundation for Program of Science and Technology Research (grant No. 2017B030314057), the Key Research Program of Frontier Sciences, CAS (QYZDJ-SSW-DQC018), and the State Key Laboratory of Organic Geochemistry, GIGCAS (grant nos. SKLOG 2020-4 and - SKLOG 2020-7). This is contribution No.IS-2937 from GIGCAS.

Appendix A. Supplementary data

Supplementary data to this article can be found online at https://doi.org/10.1016/j.chemosphere.2020.128950.

References

Abbasi, G., Li, L., Breivik, K., 2019. Global historical stocks and emissions of PBDEs. Environ. Sci. Technol. 53, 6330–6340.
Bendig, P., Vetter, W., 2010. Photolytical transformation rates of individual polybrominated diphenyl ethers in technical octabromo diphenyl ether (DE-79). Environ. Sci. Technol. 44, 1650–1655.
Bendig, P., Vetter, W., 2013. UV-induced formation of bromophenols from polybrominated diphenyl ethers. Environ. Sci. Technol. 47, 3665–3670.
Besis, A., Samara, C., 2012. Polybrominated diphenyl ethers (PBDEs) in the indoor and outdoor environments - a review on occurrence and human exposure. Environ. Pollut. 169, 217–229.
Commission, E, 2017. Proposal for a COUNCIL DECISION: on the Position to Be Adopted, on Behalf of the European Union, at the Eighth Conference of the Parties to the Stockholm Convention on Persistent Organic Pollutants Regarding the Proposals for Amendments of Annexes A and C." 2017/0058 (NLE).
de Wit, C.A., 2002. An overview of brominated flame retardants in the environment. Chemosphere 46, 583–624.
Elsner, M., Zwank, L., Hunkeler, D., Schwarzenbach, R.P., 2005. A new concept linking observable stable isotope fractionation to transformation pathways of organic pollutants. Environ. Sci. Technol. 39, 6896–6916.
Fang, L., Huang, J., Yu, G., Wang, L., 2008. Photochemical degradation of six polybrominated diphenyl ether congeners under ultraviolet irradiation in hexane. Chemosphere 71, 258–267.
Feo, M.L., Gonzalez, O., Baron, E., Casado, M., Pina, B., Esplugas, S., Eljarrat, E., Barcelo, D., 2014. Advanced UV/H2O2 oxidation of deca-bromo diphenyl ether in sediments. Sci. Total Environ. 479, 17–20.
Gandhi, N., Gewurtz, S.B., Drouillard, K.G., Kolic, T., MacPherson, K., Reiner, E.J., Bhavsar, S.P., 2017. Polybrominated diphenyl ethers (PBDEs) in Great Lakes fish: levels, patterns, trends and implications for human exposure. Sci. Total Environ. 576, 907–916.
Jarman, W.M., Hilkert, A., Bacon, C.E., Collister, J.W., Ballschmiter, K., Risebrough, R.W., 1998. Compound-specific carbon isotopic analysis of aroclors, clophens, kaneclors, and phenoclors. Environ. Sci. Technol. 32 (6), 833–836.
Li, W.L., Ma, W.L., Jia, H.L., Hong, W.J., Moon, H.B., Nakata, H., Minh, N.H., Sinha, R.K., Chi, K.H., Kannan, K., Sverko, E., Li, Y.F., 2016. Polybrominated diphenyl ethers (PBDEs) in surface soils across five asian countries: levels, spatial distribution, and source contribution. Environ. Sci. Technol. 50, 12779–12788.
Li, X.H., Tian, Y., Zhang, Y., Ben, Y.J., Lv, Q.X., 2017. Accumulation of polybrominated diphenyl ethers in breast milk of women from an e-waste recycling center in China. J. Environ. Sci-China. 52, 305–313.
Mas, S., de Juan, A., Lacorte, S., Tauler, R., 2008. Photodegradation study of decabromodiphenyl ether by UV spectrophotometry and a hybrid hard- and soft-modelling approach. Anal. Chim. Acta 618, 18–28.
Morris, A.D., Muir, D.C.G., Solomon, K.R., Teixeira, C.F., Duric, M.D., Wang, X.W., 2018. Bioaccumulation of polybrominated diphenyl ethers and alternative halogenated flame retardants in a vegetation-caribou-wolf food chain of the Canadian arctic. Environ. Sci. Technol. 52, 3136–3145.
Pan, Y.H., Tsang, D.C.W., Wang, Y.Y., Li, Y., Yang, X., 2016. The photodegradation of polybrominated diphenyl ethers (PBDEs) in various environmental matrices: kinetics and mechanisms. Chem. Eng. J. 297, 74–96.
Rosenfelder, N., Bendig, P., Vetter, W., 2011. Stable carbon isotope analysis (delta^{13}C values) of polybrominated diphenyl ethers and their UV-transformation products. Environ. Pollut. 159, 2706–2712.
Schmidt, T.C., Zwank, L., Elsner, M., Berg, M., Meckenstock, R.U., Haderlein, S.B., 2004. Compound-specific stable isotope analysis of organic contaminants in natural environments: a critical review of the state of the art, prospects, and future challenges. Anal. Bioanal. Chem. 378, 283–300.
Usenko, C.Y., Robinson, E.M., Usenko, S., Brooks, B.W., Bruce, E.D., 2011. Pbde developmental effects on embryonic zebrafish. Environ. Toxicol. Chem. 30, 1865–1872.
Vetter, W., Gaul, S., Armbruster, W., 2008. Stable carbon isotope ratios of POPS– A tracer that can lead to the origins of pollution. Environ. Int. 34 (3), 357–362.
Wang, G.G., Peng, J.L., Zhang, D.H., Li, X.G., 2016. Characterizing distributions, composition profiles, sources and potential health risk of polybrominated diphenyl ethers (PBDEs) in the coastal sediments from East China Sea. Environ. Pollut. 213, 468–481.
Wang, R., Tang, T., Xie, J.B., Tao, X.Q., Huang, K.B., Zou, M.Y., Yin, H., Dang, Z., Lu, G.N., 2018a. Debromination of polybrominated diphenyl ethers (PBDEs) and their conversion to polybrominated dibenzofurans (PBDFs) by UV light: mechanisms and pathways. J. Hazard Mater. 354, 1–7.
Wang, Y.F., Zhu, H.W., Wang, Y., Zhang, X.L., Tam, N.F.Y., 2018b. Diversity and dynamics of microbial community structure in different mangrove, marine and freshwater sediments during anaerobic debromination of PBDEs. Front. Microbiol. 9.
Wei, H., Zou, Y.H., Li, A., Christensen, E.R., Rockne, K.J., 2013. Photolytic debromination pathway of polybrominated diphenyl ethers in hexane by sunlight. Environ. Pollut. 174, 194–200.

Zakon, Y., Halicz, L., Gelman, F., 2013. Bromine and carbon isotope effects during photolysis of brominated phenols. Environ. Sci. Technol. 47, 14147–14153.
Zelmer, A., Zhang, N., Kominkova, K., Nachtigallova, D., Richnow, H.H., Klan, P., 2015. Photochemistry of 4-chlorophenol in liquid and frozen aqueous media studied by chemical, compound-specific isotope, and DFT analyses. Langmuir 31, 10743–10750.
Zhao, Q., Zhao, H.M., Quan, X., He, X., Chen, S., 2015. Photochemical formation of hydroxylated polybrominated diphenyl ethers (OH-PBDEs) from polybrominated diphenyl ethers (PBDEs) in aqueous solution under simulated solar light irradiation. Environ. Sci. Technol. 49, 9092–9099.